VIP Light-Emitting Diodes

DOI: 10.1002/anie.200604240

Highly Efficient, Near-Infrared Electrophosphorescence from a Pt–Metalloporphyrin Complex**

Carsten Borek, Kenneth Hanson, Peter I. Djurovich, Mark E. Thompson, Kristen Aznavour, Robert Bau, Yiru Sun, Stephen R. Forrest, Jason Brooks, Lech Michalski, and Julie Brown*

Organic light-emitting diodes (OLEDs) have been the subject of a significant research effort for the past two decades with a focus on devices that emit almost exclusively in the visible part of the electromagnetic spectrum.[1] Recently, there has been a growing interest in OLEDs that emit in the near-infrared (NIR) region (700–2500 nm).[2–4] Applications for these NIR OLEDs are particularly interesting for night-vision-readable displays[5] and sensors.[6] The efficiency of OLEDs are markedly improved when fluorescent emissive dopants are replaced with phosphorescent heavy-metal complexes that can effectively harvest both the singlet and triplet excitons formed in electroluminescence, with wavelengths (λ) ranging from the near-ultraviolet into the red (with peak emission at $\lambda_{max} = 380$–650 nm).[7–10] Herein, we report on an efficient NIR OLED that utilizes a phosphorescent Pt–metalloporphyrin dopant, with an external quantum efficiency (EQE) greater than 6% at $\lambda_{max} = 765$ nm and a full width at half maximum of 31 nm (500 cm^{-1}).

Previously, two classes of phosphorescent complexes have been employed as dopants in NIR-emitting OLEDs. The first utilizes trivalent lanthanide cations (Ln^{3+}) as the emitting centers, for example, Er^{3+} or Nd^{3+}, chelated with chromophoric ligands to sensitize excitation-energy transfer to the lanthanide ion.[11] Schanze et al. have reported an NIR OLED utilizing Ln^{3+} in conjunction with a porphyrin/polystyrene matrix, with EQE ranging from 8.0×10^{-4} to 2.0×10^{-4}% at approximately 1 mA cm^{-2}.[5] Similarly, a Nd(phenalenone)$_3$-based OLED had an EQE of 0.007% at $\lambda_{max} = 1065$ nm.[4] The second class of NIR OLEDs is transition-metal complexes, similar to those used in the visible region. A recent report of an electrophosphorescent device that used a cyclometalated [(pyrenyl–quinolyl)$_2$Ir(acac)] complex as the phosphor gave $\lambda_{max} = 720$ nm and an EQE of 0.1%.[6]

A family of complexes that have shown intense absorption and emission in the red-to-NIR region of the spectrum are the metalloporphyrins.[12,13] There are a number of reports of OLEDs fabricated with [Pt(oep)], [Pt(tpp)] (oep = 2,3,7,8,12,13,17,18-ocatethylporphryin, tpp = 5,10,15,20-tetraphenylporphyrin), or analogues of these compounds as phosphorescent emitters, with emission maxima between 630 and 650 nm,[7,14–22] however, there has been no apparent effort to shift the Pt–porphyrin-based OLED emission into the NIR region. Porphyrin chromophores with fused aromatic moieties at the β-pyrrole positions, for example, tetrabenzoporphyrin (bp), exhibit a bathochromic shift (relative to unsubstituted porphyrin) of the absorption and emission energy, owing to the expansion of the π-electronic system of the porphyrin core.[23] The addition of bulky groups to the meso positions of the porphyrin macrocycles with β-substituted pyrroles leads to the formation of nonplanar porphyrins, and further red-shifts the absorption spectra.[24] Coordination of a heavy-metal atom increases the rate of the intersystem crossing between singlet and triplet states of the metalloporphyrins, thereby enhancing the rate of radiative decay from the triplet state. For these reasons, we focus here on Pt^{II}–tetraphenyltetrabenzoporphyrin, [Pt(tpbp)] (Figure 1), as a phosphorescent dopant.

Analysis of the [Pt(tpbp)] complex by X-ray crystallography reveals a nonplanar molecular structure with a saddle-type distortion, similar to that found in other tpbp derivatives.[25] Crystallographic data are available in the Supporting Information and from the Cambridge Crystallographic Data Centre (CCDC-627735).[26] An analysis of [Pt(tpbp)] using normal-coordinate structural decomposition (NSD) software[27,28] quantifies the various distortions that accompany the macrocyclic deformation (Figure 1, top). The total out-of-plane distortion ($D_{oop} = 2.83$ Å) is almost exclusively described by saddling (B2u = 2.83 Å), while doming (A2u = 0.045 Å), wave x and wave y deformations (similar to a chair conformation in cyclohexane, in either the x or y direction; Eg = 0.042 and 0.068 Å, respectively), propellering (A1u = 0.0003 Å), and ruffling (B1u = 0.006 Å) contribute

[*] C. Borek, K. Hanson, Dr. P. I. Djurovich, Prof. M. E. Thompson, K. Aznavour, Prof. R. Bau
Department of Chemistry
University of Southern California
Los Angeles, CA 99089 (USA)
Fax: (+1) 213-740-8594
E-mail: met@usc.edu

Y. Sun
Department of Electrical Engineering
Princeton University
Princeton, NJ 08544 (USA)

Prof. S. R. Forrest
Department of Electrical Engineering and Computer Science and Department of Physics
University of Michigan
Ann Arbor, MI 48109 (USA)

Dr. J. Brooks, L. Michalski, Dr. J. Brown
Universal Display Corporation
Ewing, NJ 08618 (USA)

[**] The authors acknowledge financial support from the U.S. Dept. of the Army, CECOM for the phase II SBIR program (contract no. W15P7T-06-C-T201), and Universal Display Corporation.

Supporting information for this article, including the procedure used to prepare and purify [Pt(tpbp)], details of the crystallographic work, NSD analysis, and the methods used to prepare and test OLEDs, is available on the WWW under http://www.angewandte.org or from the author.

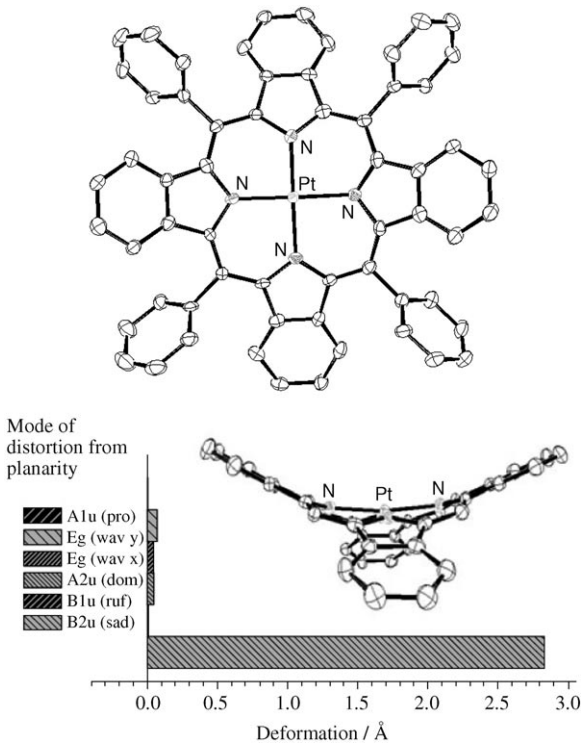

Figure 1. Crystal structure of [Pt(tpbp)]. Top: top view; bottom: edge view (*meso*-phenyl substituents removed for clarity) with results of NSD analysis.

only slightly to the nonplanarity. This distortion is greater than that found in [Zn(tpbp)] ($D_{oop} = 2.35$ Å),[25] yet is less than that of a [Ni(tpbp($CO_2Me)_8$)] derivative ($D_{oop} = 3.43$ Å).[23]

Electrochemical analysis of [Pt(tpbp)], versus an internal ferrocene reference, shows a reversible oxidation at 0.24 V and quasireversible reduction at −1.85 V. The highest occupied (HOMO) and the lowest unoccupied (LUMO) molecular orbitals calculated from these data are 4.9 and 2.5 eV in energy relative to vacuum, respectively.[29] The absorption spectrum (Figure 2) displays strong transitions for the Soret band at $\lambda_{max} = 430$ nm, with an extinction coefficient of

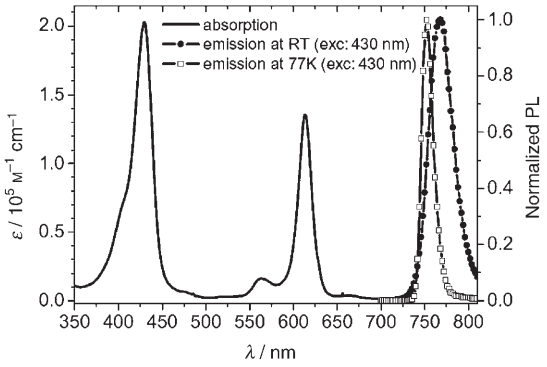

Figure 2. Room-temperature absorption spectrum (solid line), and normalized emission spectra at room temperature (closed circles) and at 77 K (open squares) of [Pt(tpbp)] in 2-methyl-THF.

$\varepsilon_{430nm} = 2.03 \times 10^5\ M^{-1}\,cm^{-1}$, and the Q band with $\lambda_{max} = 611$ nm ($\varepsilon_{611nm} = 1.35 \times 10^5\ M^{-1}\,cm^{-1}$), which differ slightly from the values for the analogous [Pd(tpbp)] complex.[30]

The phosphorescence spectrum of thoroughly degassed [Pt(tpbp)] has $\lambda_{max} = 765$ nm, with a transient lifetime of $\tau = 53$ μs at room temperature (298 K); these values shift to $\lambda_{max} = 751$ nm and $\tau = 73$ μs at 77 K. The blue shift is due to a rigidochromic effect at low temperature. Assuming that the radiative rate constant does not show a temperature dependence between 298 K and 77 K, and the nonradiative decay rate is negligible at 77 K, the ratio of the lifetimes gives the photoluminescence (PL) efficiency. The photophysical properties of Pt–tetrabenzoporphrin [Pt(bp)] support these assumptions.[31] The photoluminescent quantum yield (Φ_{PL}) estimated by this method is 0.7. Radiative ($k_r = 1.3 \times 10^4\ s^{-1}$) and nonradiative ($k_{nr} = 5.8 \times 10^3\ s^{-1}$) decay rates were estimated from the lifetime (τ) data ($k_r = 1/\tau_{77K}$; $k_{nr} = 1/\tau_{298K} - k_r$). The nonradiative rate is similar to that reported for [Pd(tpbp)] ($k_{nr} = 4.2 \times 10^3\ s^{-1}$), but the stronger spin–orbit coupling of Pt significantly increases the radiative rate (compare [Pd(tpbp)]: $k_r = 8.8 \times 10^2\ s^{-1}$).[30]

To minimize concentration quenching in [Pt(tpbp)]-based OLEDs, [Pt(tpbp)] was doped into a tris(8-hydroxyquinoline)aluminum (Alq_3) host.[7] The dopant singlet and triplet levels fall well below those of Alq_3 ($S_1 = 500$ nm, $T_1 = 590$ nm).[32] The OLEDs prepared here incorporated a neat Alq_3 exciton-blocking layer (EBL) to prevent exciton quenching at the cathode surface. Thus, the structure used was: ITO/(400 Å) NPD/(400 Å) Alq_3 + 6 wt% [Pt(tpbp)]/(500 Å) Alq_3/(10 Å) LiF/(1100 Å) Al (ITO = indium tin oxide, NPD = *N*,*N*′-bis(1-naphthyl)-*N*,*N*′-diphenyl-1,1′-biphenyl-4,4′-diamine), hereafter referred to as device 1. This device has an EQE of 6.3% at 0.1 mA cm^{-2}, which gradually decreases as the current density is increased (Figure 3). The intensity is roughly 0.1 μW cm^{-2} at 3 V and 750 μW cm^{-2} at 12 V. The electroluminescence (EL) spectrum for device 1 displays strong NIR emission at 769 nm, with no Alq_3 signal (520 nm) at any bias level (Figure 3), thus indicating complete energy transfer from host to guest.

Devices were also prepared to test the operational stability of [Pt(tpbp)]-based OLEDs. For these tests, the following structure (device 2) was used: ITO/(400 Å) NPD/(300 Å) Alq_3 + 6 wt% [Pt(tpbp)]/(400 Å) BAlq/(10 Å) LiF/(1000 Å) Al, where BAlq is aluminum(III) bis(2-methyl-8-quinolinato)4-phenylphenolate, and serves as the exciton-blocking layer. The charge transport, blocking, and host materials have previously been demonstrated to give high efficiencies and long electrophosphorescent device lifetimes.[33,34] At a low current density of 0.1 mA cm^{-2}, device 2 has a maximum EQE of 3%, falling to 1.1% at 10 mA cm^{-2} (Figure 3). The electroluminscence spectrum is identical to that for device 1.

The device was aged at a high constant current of 40 mA cm^{-2} corresponding to an initial intensity of 740 μW cm^{-2}. The data in Figure 4 (see inset) suggest that device 2 will maintain greater than 90% of its initial intensity after 1000 h of operation. A 0.5-V rise in voltage occurring during the first 50 h corresponds to the initial fast decay in device intensity. After 100 h, the voltage stabilizes at 13.3 V.

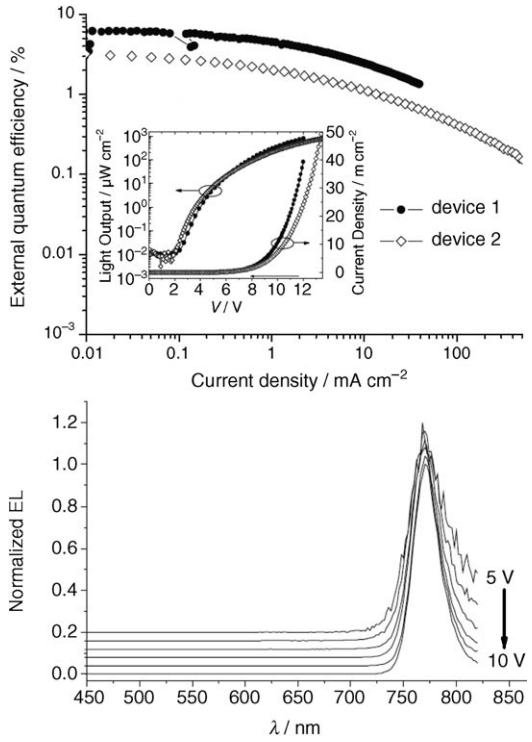

Figure 3. Top: external quantum efficiency versus current density. Device 1: ITO / (400 Å) NPD / (400 Å) Alq_3 + 6 wt% [Pt(tpbp)] / (500 Å) Alq_3 / (10 Å) LiF / (1100 Å) Al; device 2: ITO / (400 Å) NPD / (300 Å) Alq_3 + 6 wt% [Pt(tpbp)] / (400 Å) BAlq / (10 Å) LiF / (1000 Å) Al. Inset: Intensity and current density versus voltage for devices 1 and 2. Bottom: normalized electroluminescence spectra for device 1 at 5 V to10 V, in 1-V steps. Spectra offset for clarity.

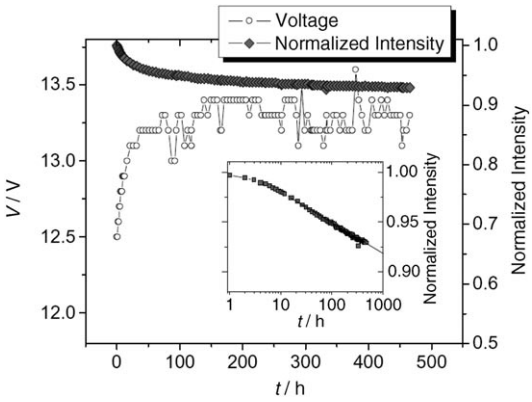

Figure 4. Intensity versus operating time, normalized to initial intensity (closed squares) and voltage (open circles). The initial intensity was 740 μW cm^{-2}. The inset shows the time versus radiance data plotted on a semilogarithmic scale with extrapolation to 1000 h.

The operating voltage is sensitive to variations in temperature, which may account for some of the observed fluctuation. These initial results demonstrate that [Pt(tpbp)] devices are stable at high drive currents, although further study is needed to determine the device lifetime at radiances suitable for display use, assuming the viewer is using night-vision goggles. The long device lifetimes estimated for [Pt(tpbp)]-based OLEDs are consistent with the previously reported lifetime for [Pt(oep)]-based OLEDs ($> 10^6$ h measured at low luminance),[35] thus illustrating the high device stability of Pt–porphyrin-based OLEDs.

In conclusion, we have demonstrated highly efficient NIR electrophosphorescent devices utilizing [Pt(tpbp)] emitters with a device peak EQE of 6.3 % at 0.1 mA cm^{-2}, and lifetime of greater than 1000 h to 90 % efficiency at 40 mA cm^{-2}. The very high efficiencies of the NIR devices make them suitable for many night-vision display and sensing applications. Achieving even longer-wavelength emission is possible by extending the conjugation length of the ligand structure.

Received: October 17, 2006
Published online: January 9, 2007

Keywords: luminescence · near-infrared emission · OLEDs · phosphorescence · porphyrinoids

[1] Z. H. Kafafi, *Organic Electroluminescence*, CRC, Boca Raton, **2005**.
[2] B. S. Harrison, *Appl. Phys. Lett.* **2001**, *79*, 3770.
[3] L. H. Slooff, A. Polman, F. Cacialli, *Appl. Phys. Lett.* **2001**, *78*, 2122.
[4] A. O'Riordan, E. O'Connor, S. Moynihan, P. Nockemann, P. Fias, R. Van Deun, D. Cupertino, P. Mackie, G. Redmond, *Thin Solid Films* **2006**, *497*, 299.
[5] K. S. Schanze, J. R. Reynolds, J. M. Boncella, B. S. Harrison, T. J. Foley, M. Bouguettaya, T.-S. Kang, *Synth. Met.* **2003**, *137*, 1013.
[6] E. L. Williams, J. Li, G. E. Jabbour, *Appl. Phys. Lett.* **2006**, *89*, 083506.
[7] M. A. Baldo, D. F. O'Brien, Y. You, A. Shoustikov, S. Sibley, M. E. Thompson, S. R. Forrest, *Nature* **1998**, *395*, 151.
[8] S. Lamansky, P. Djurovich, D. Murphy, F. Abdel-Razzaq, H. E. Lee, C. Adachi, P. E. Burrows, S. R. Forrest, M. E. Thompson, *J. Am. Chem. Soc.* **2001**, *123*, 4304.
[9] E. Holder, B. M. W. Langeveld, U. S. Schubert, *Adv. Mater.* **2005**, *17*, 1109.
[10] R. J. Holmes, S. R. Forrest, T. Sajoto, A. Tamayo, P. I. Djurovich, M. E. Thompson, J. Brooks, Y. J. Tung, B. W. D'Andrade, M. S. Weaver, R. C. Kwong, J. J. Brown, *Appl. Phys. Lett.* **2005**, 87.
[11] J. Kido, Y. Okamoto, *Chem. Rev.* **2002**, *102*, 2357.
[12] K. Kalyanasundaram, *Photochemistry of Polypyridine and Porphyrin Complexes*, Academic Press, London, **1992**.
[13] T. V. Duncan, K. Susumu, L. E. Sinks, M. J. Therien, *J. Am. Chem. Soc.* **2006**, *128*, 9000.
[14] D. F. O'Brien, M. A. Baldo, M. E. Thompson, S. R. Forrest, *Appl. Phys. Lett.* **1999**, *74*, 442.
[15] M. Colle, C. Garditz, M. Braun, *J. Appl. Phys.* **2004**, *96*, 6133.
[16] H. D. F. Burrows, M. , J. S. de Melo, A. P. Monkman, S. Navaratnam, *J. Am. Chem. Soc.* **2003**, *125*, 15310.
[17] Y. Wang, *Appl. Phys. Lett.* **2004**, *85*, 4848.
[18] V. A. Montes, C. Perez-Bolivar, N. Agarwal, J. Shinar, P. Anzenbacher, *J. Am. Chem. Soc.* **2006**, *128*, 12436.
[19] M. Ikai, F. Ishikawa, N. Aratani, A. Osuka, S. Kawabata, T. Kajioka, H. Takeuchi, H. Fujikawa, Y. Taga, *Adv. Funct. Mater.* **2006**, *16*, 515.
[20] L. Yanqin, R. Aurora, S. Marco, M. Marco, H. Cheng, W. Yue, L. Kechang, C. Roberto, G. Giuseppe, *Appl. Phys. Lett.* **2006**, *89*, 061125.
[21] Q. Hou, Y. Zhang, F. Li, J. Peng, Y. Cao, *Organometallics* **2005**, *24*, 4509.
[22] J. Kalinowski, W. Stampor, J. Szmytkowski, M. Cocchi, D. Virgili, V. Fattori, P. D. Marco, *J. Chem. Phys.* **2005**, *122*, 154710.

[23] V. V. Rozhkov, M. Khajehpour, S. A. Vinogradov, *Inorg. Chem.* **2003**, *42*, 4253.
[24] O. S. Finikova, S. E. Aleshchenkov, R. P. Brinas, A. V. Cheprakov, P. J. Carroll, S. A. Vinogradov, *J. Org. Chem.* **2005**, *70*, 4617.
[25] R.-J. Cheng, Y.-R. Chen, S. L. Wang, C. Y. Cheng, *Polyhedron* **1993**, *12*, 1353.
[26] http://www.ccdc.cam.ac.uk/data_request/cif.
[27] W. Jentzen, X.-Z. Song, J. A. Shelnutt, *J. Phys. Chem. B* **1997**, *101*, 1684.
[28] http://jasheln.unm.edu/jasheln/content/nsd/nsd_welcome.htm.
[29] B. W. D'Andrade, S. Datta, S. R. Forrest, P. Djurovich, E. Polikarpov, M. E. Thompson, *Org. Electron.* **2005**, *6*, 11.
[30] J. E. Roger, K. A. Nguyen, D. C. Hufnagle, D. G. McLean, W. Su, K. M. Gossett, A. R. Burke, S. A. Vinogradov, R. Patcher, P. A. Fleitz, *J. Phys. Chem. A* **2003**, *107*, 11331.
[31] T. J. Aartsma, M. Gouterman, C. Jochum, A. L. Kwiram, B. V. Pepich, L. D. Williams, *J. Am. Chem. Soc.* **1982**, *104*, 6278.
[32] W. Humbs, E. van Veldhoven, H. Zhang, M. Glasbeek, *Chem. Phys. Lett.* **1999**, *304*, 10.
[33] R. C. Kwong, M. R. Nugent, L. Michalski, T. Ngo, K. Rajan, Y.-J. Tung, M. S. Weaver, T. X. Zhou, M. Hack, M. E. Thompson, S. R. Forrest, J. J. Brown, *Appl. Phys. Lett.* **2002**, *81*, 162.
[34] R. C. Kwong, M. S. Weaver, M.-H. M. Lu, Y.-T. Tung, A. B. Chwang, T. X. Zhou, M. Hack, J. J. Brown, *Org. Electron.* **2003**, *4*, 155.
[35] P. E. Burrows, S. R. Forrest, T. X. Zhou, L. Michalski, *Appl. Phys. Lett.* **2000**, *76*, 2493.

